de Brito Sá, Égil; Rodríguez Santiago, Luis; Sodupe Roure, Mariona; [et al.]. «Influence of ligands and oxidation state on the reactivity of pentacoordinated iron carbenes with olefins : metathesis versus cyclopropanation». Organometallics, Vol. 37, issue 8 (April 2018), p. 1229-1241. DOI 10.1021/acs.organomet.7b00786

Influence of ligands and oxidation state on the reactivity of pentacoordinated iron carbenes with olefins: metathesis *versus* cyclopropanation

Égil de Brito Sá,[a,b] Luis Rodríguez-Santiago,[a] Mariona Sodupe,[a]
Xavier Solans-Monfort[a,*]

[a]Departament de Química, Universitat Autònoma de Barcelona, 08193 –
Bellaterra, Spain

[b]Universidade Federal do Piauí, *Campus* Ministro Reis Velloso, 64202-020 –
Parnaíba-Piauí, Brazil

Abstract

DFT (OPBE) calculations have been used to explore how the nature of the ligands, the coordination around the metal center and the formal iron oxidation state tunes the ground state multiplicity of $L_4Fe{=}CH_2$ carbenes and influences their reactivity with olefins. The study is focused on the competition between olefin metathesis and alkene cyclopropanation. We examined carbenes bearing ligands, which are already used in iron complexes, as well as other *in-silico* designed species in order to analyze borderline cases. For each complex, the three potential spin states (singlet (S=0), triplet (S=1) and quintet (S=2)) of the carbene, metallacyclobutane and metal fragment arising from cyclopropanation have been considered. Results show that the addition of σ-donating groups leads to singlet ground state iron carbenes and, although for the majority of cases of formally Fe(II) species the resulting metallacyclobutane intermediates presents a triplet ground state, the presence of a weak σ-donating ligand *trans* to the carbene combined with donating groups *cis* to the carbene can lead to Fe(II) complexes with thermodynamic properties close to those of the Ru-based Grubbs catalyst. Furthermore, the reduction of the metal center, to formally Fe(0) species implies significant changes in the energetics: the carbene and metallacyclobutane species present a singlet ground state and the alkene cyclopropanation becomes unfavorable in the singlet state. However, the energy barriers that have to be overcome in the olefin metathesis reaction with our selected candidates are higher than those for cyclopropanation. For the case of the Fe(II) with weak ligands *trans* to the carbene, this arises from the fact that the cycloreversion *trans* to this ligand is not favorable. On the other hand, the Fe(0) pentacoordinated carbenes are formally eighteen electron complexes and thus, the coordination of the olefin is hindered. Therefore, these species would only be potentially active with the use of labile ligands that decoordinate in the presence of the incoming olefin. Overall, it was found that the set of ligands that leads to the appropriate thermodynamics seems to be specific for each coordination number and oxidation state.

Introduction

Olefin metathesis is a versatile reaction that allows the synthesis of a large variety of unsaturated products by formal alkylidene-end exchange between different alkene molecules (Scheme 1a).[1–3] It has been applied to the synthesis of polymers, drugs, natural products and in the conversion of biomass into fuels.[4–7] The reaction only takes place in the presence of a metal carbene that acts as catalyst. According to Chauvin's mechanism,[2,8] the reaction involves the formation of metallacyclobutanes, which are the key reaction intermediates (Scheme 1b). The most common catalysts for olefin metathesis are based on Mo, W[3,9–12] and Ru.[1,13–18] They have been largely used and outstanding results have been obtained.

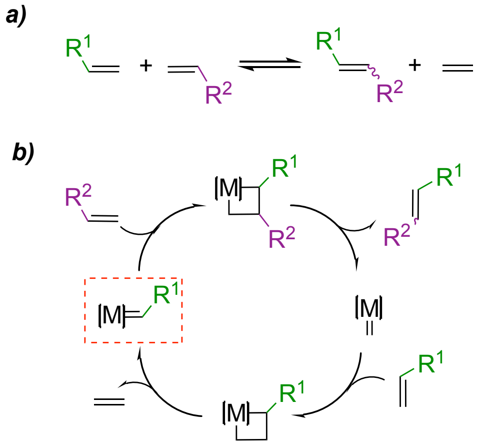

Scheme 1.

Lower, but still appreciable catalytic activity has been observed for carbene complexes of other metals.[5,19–22] In this context, the use of more abundant Fe, Co, Ni based carbenes is a desirable goal in terms of sustainability, since complexes of Fe, Co and Ni are usually cheaper and less toxic.[23,24] However, to the best of our knowledge, there are very few existing examples of first row transition metal carbene complexes able to perform the alkene metathesis reaction.[5,19,20,22] They are based on Ti[22] and V[5,19,20] and the scope of the reactions in which they have been applied is still rather limited. Iron complexes appear as an interesting alternative, since iron belongs to the same group of ruthenium and it is the earth most abundant transition metal. Unfortunately, the synthesis of iron-carbenes is challenging[25] and, consequently, the literature about such complexes is very limited. Furthermore these existing examples usually undergo alkene cyclopropanation or radical reactions when reacting with olefins.[26–28] In this context, several difficulties can be easily identified when designing an iron carbene able to catalyze olefin metathesis. First, the M=CR_2 carbene bond tends to be weaker for 3d metal containing complexes than for 4d and 5d metal species.[29] This decreases the metal carbene stability and favor the alkene cyclopropanation and other carbene transfer reactions. [30–42] Second, while 4d and 5d metal complexes usually present a singlet ground state, several spin states may be close in energy in first row transition metal carbenes. This includes open shell systems that would more easily proceed through radical reactions.

Computational chemistry can be used as a complementary tool to explore and rationalize the influence of the nature of the ligands, the coordination number and the metal cation formal oxidation state on the ground state multiplicity of the metal carbene, the metal-carbene bond strength and the reactivity of these species towards olefins. The properties of hypothetical iron carbene complexes and their reactivity towards olefins were analyzed in few previous computational studies.[29,43–48] Eisenstein *et al.* performed extended Hückel calculations on $L_4Fe=CH_2$ and $Cp_2Fe=CH_2$ iron containing complexes.[43] Poater et al.[46,47] and Vasiliu et al.[29] analyzed the effect of substituting the ruthenium center by iron in the most common $L_2Cl_2Ru=CR_2$ Grubbs type catalysts. Finally, we have recently analyzed how the nature of the ligands and the geometry around the metal center can tune the properties of $L_3Fe=CH_2$ in a way that the carbene and the metallacyclobutane intermediate presents a singlet ground state and the alkene cyclopropanation is disfavored.[44]

In the study reported here, we extend our previous work[44] to pentacoordinated $L_4Fe=CH_2$ complexes. We focus on how the nature of the ligands (flexibility and σ-donating ability) and the formal oxidation state of iron can favor the formation of a singlet carbene and metallacycle as well as disfavor the alkene cyclopropanation. In order to achieve this goal, we computed all potential spin states of the metal carbene complex, the metallacyclobutane intermediate and the metal fragment resulting from alkene cyclopropanation. For the sake of simplicity, the carbene is represented as $Fe=CH_2$ and the reacting olefin as ethene. We first analyze the electronic structure and energetics of an initial set of Fe(II) carbenes (the carbene is counted as a neutral ligand) mainly based on existing ligands and, afterwards, we analyze the effect of modifying the chelating ligand rigidity, the σ-donating ability of the ligands and metal reduction to Fe(0) by *in-silico* modifications to this first set of species. Results show that there are different ways for stabilizing the singlet state of the carbene and metallacyclobutane intermediate and disfavor alkene cyclopropanatiion, the most efficient strategy strongly depends on the coordination number, the nature of the ligands around the metal center and its formal oxidation state.

Computational details

All calculations were performed with the OPBE density functional.[49–51] The geometries were optimized in the gas phase without any geometrical constraint. Main group elements were represented with the valence double-ζ plus polarization 6-31G(d,p)[52,53] basis set and iron with the Wachters-Hay valence triple-ζ plus polarization basis set enlarged with diffuse functions, 6-311+G(d,p).[53,54] Calculations for open-shell systems were carried out considering the spin-unrestricted formalism. The possibility of a low lying open-shell singlet state was also explored for some selected species, starting from the optimized triplet state structure. However, in all cases, the optimization collapsed to the closed shell solution. The nature of all stationary points was verified by vibrational analysis. The final energetics was obtained by single point calculations employing the 6-311++G(d,p)[53,55] basis set for main group elements and the same basis sets used in the optimizations for iron. All the values reported as (G_{gp} + D2) are based on gas phase Gibbs energies (G_{gp}), in which the thermal corrections were obtained at 298.15 K and 1 atm with the smallest basis set, plus Grimme's (D2) correction for the dispersion forces. The Grimme's contribution is evaluated at the optimized geometry using the S_6 scaling factor for the PBE functional (0.75).[56] All calculations were performed with the Gaussian09 package.[57] The Natural Bond Orbital (NBO)[58] and Atoms in Molecules (AIM)[59] analyses were used for the rationalization of the electronic structure. Associated Cartesian coordinates of all optimized structures are given in the electronic supporting information (ESI).

It is worth mentioning that OPBE has been shown to properly describe energy differences between spin states of iron metal complexes.[60–62] This level of theory was used in our previous works and it reproduced the ground spin state of several existing iron carbenes as well as their preferred reactivity.[44,63] However, in order to evaluate the suitability of OPBE functional in properly describing reaction thermodynamics, we have also performed calculations for some representative cases with B3LYP, a highly tested functional for organometallic reactions. Results are reported in Table S1 of the Supporting Information. First, regarding the spin multiplicity of the ground state of the different considered species, B3LYP, as expected,[61,64] tends to overstabilize the triplet state in all cases. Concerning the thermodynamics, B3LYP-D2 tends to destabilize both the metallacyclobutane and the cyclopropanation products by around 5-7 kcal mol^{-1} with respect to the isolated reactants, when compared to OPBE-D2 results. Since the obtained trends are similar for the two functionals, the choice of the functional does not affect the conclusions drawn in the work and the less time consuming OPBE functional was used.

Results and discussion

The goal of this work is analyzing how the nature of the ligands (rigidity and σ-donating ability) and the formal oxidation state of the metal cation influences the electronic ground state of the metal carbene, the Fe=CH$_2$ bond strength and their reactivity towards olefins. For that, we first analyze a set of initial Fe(II) species mainly constructed considering ligands that have already been used for synthetizing first row transition metal complexes. After that, we expand the study to other *in-silico* designed ligands that represent borderline cases. Finally, we explore the effect of metal reduction to formally Fe(0). In each case, we focus firstly on the electronic structure of the carbene and in a second stage we discuss its reactivity towards olefins. Results are compared to the values computed in our previous work for the ruthenium based second-generation Grubbs active species (**0** in Scheme 2).[44] In the last part of the results and discussion section, the energetics of the transition state structures for alkene metathesis and alkene cyclopropanation of representative complexes showing thermodynamics close to those of **0** are discussed.

Initial set of carbenes. Complexes belonging to the first set of species are schematically shown in Scheme 2. Complexes **1** to **4** are based on ligands that are already used in the synthesis of first row metal complexes. The ligands of complex **1**[65] and **2**,[66] were used by Costas and co-workers for the synthesis of high oxidation state iron oxo complexes.[67] Furthermore, it was suggested that a carbene, whose structure is similar to the one labeled as **1** in Scheme 2 is involved in the carbene insertion in C-H bonds of arenes.[42] The ligand of complex **3** is a variation of the Scorpionato motive[68] in which the central boron is replaced by a triethyleneamine linker.[69,70] A similar ligand with mesityl groups instead of phenyls was used by Meyer and co-workers for the synthesis of a high oxidation state iron nitride complex.[69] Finally, the ligand of complex **4** was used by Ribas and co-workers to synthesize a Co(III) complex catalytically active in the C-C bond formation through a metastable carbene complex.[71] In addition, two other complexes were studied in this reference set. Complex $\mathbf{3_H}$ is a modification of **3** where the phenyl groups were replaced by H atoms as N-substituents of the NHC. This was done with the aim of understanding the role of the steric effect on the relative stabilities of the different spin states and complex reactivity with olefins. Complex **5** is a variation of **1**, where one of the pyrinine-based ligands is replaced by a more σ-donating neutral NHC ligand. The geometry around the metal center in the initial carbene and the relative stabilities of the different spin states of the carbene, metallacycle and metal fragment resulting from the cyclopropanation are reported Table 1. Values for the well-known Ru-based 2nd generation Grubbs catalyst (**0**) are also reported for comparison. The optimized geometries of the structures discussed above are shown in Figures S1 to S6 of the ESI. Spin density distribution as well as the NBO and AIM analyses are shown in Table S2.

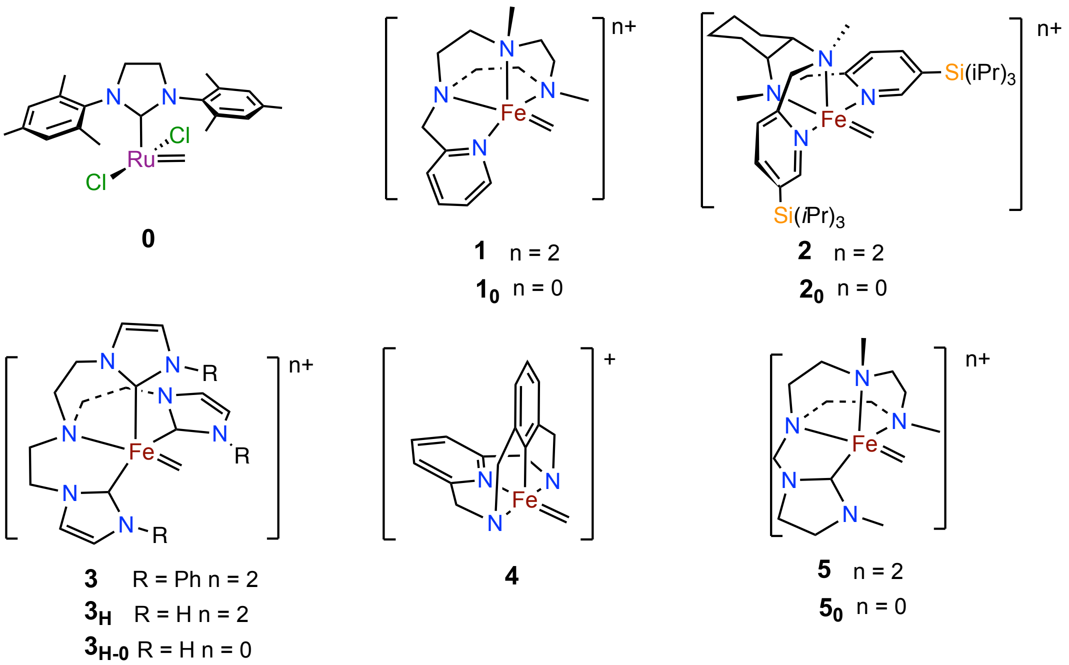

0

1 n = 2
1$_0$ n = 0

2 n = 2
2$_0$ n = 0

3 R = Ph n = 2
3$_H$ R = H n = 2
3$_{H-0}$ R = H n = 0

4

5 n = 2
5$_0$ n = 0

Scheme 2

Table 1. Relative Gibbs (G_{gp} + D2) energies of the species involved in the metathesis and cyclopropanation reactions of the Grubbs Ru complex and iron carbene complexes **1** to **5** with respect to the carbene singlet state and ethene. All values are in kcal mol^{-1}

Complex	Geometry[a]			Carbene			Metallacyclobutane			Cyclopropanation[b]		
	S=0	*S=1*	*S=2*	*S=0*	*S=1*	*S=2*	*S=0*	*S=1*	*S=2*	*S=0*	*S=1*	*S=2*
0[c]				0.0	19.5	49.1	-6.8	8.2	47.5	8.6	-7.4	9.7
1	SBP	SBP	TBP	0.0	-2.3	3.8	-20.7	-23.1	--[f]	-22.3	-28.6	-43.8
2	SBP	SBP	--[d]	0.0	-6.3	5.1	-23.4	-26.7	--[f]	-26.8	-33.2	-50.8
3	SBP	TBP	TBP	0.0	4.4	23.5	6.8	4.7	--[f]	-25.1	-30.1	N.A.
3$_H$	SBP	TBP	--[d]	0.0	7.6	22.7	-4.5	-6.0	--[f]	-18.3	-23.1	-32.1
4	SBP	SBP		0.0	12.1	--[e]	-11.7	-5.9	-7.4	-17.4	-16.5	-13.9
5	SBP	TBP		0.0	-3.9	--[e]	-15.9	-19.0	--[f]	-17.8	-25.7	-37.3

[a] Coordination around the metal center in the Fe-carbene.

[b] The cyclopropanation values correspond to the Gibbs energy difference between cyclopropanation products and initial carbene + ethene.

[c] Energies obtained for the methylidene active species of the second-generation Grubbs catalyst at the same level of calculation.

[d] The coordination around the metal center is in between the SBP and TBP ones.

[e] The Fe=CH$_2$ carbene is not a minimum of the potential energy surface, optimization leads to carbene insertion into one of the C-based ligands (see text and Table S3 of the ESI for further details).

[f] Optimizations spontaneously evolved to the formation of cyclopropane.

All singlet state carbenes present a square based pyramid (SBP) coordination around the metal center with the carbene occupying one of the basal positions. The carbene substituents are located perpendicular to the basal plane, suggesting that the Fe=C π-bond is formed by the overlap between the iron d_{xy} orbital of the basal plane and the corresponding p_y carbon orbital (Figure 1a). Indeed, the singlet state structure corresponds to a low spin SBP coordination around the metal center. The Fe=C bond distance ranges from 1.708 Å and 1.726 Å, as in the $L_3Fe{=}CH_2$ carbenes and consistent with a significant double bond character. This is further confirmed by the Wiberg bond index values obtained with NBO analysis (1.61-1.55) and the delocalization index computed with AIM (1.71-1.66) (see Table S2).

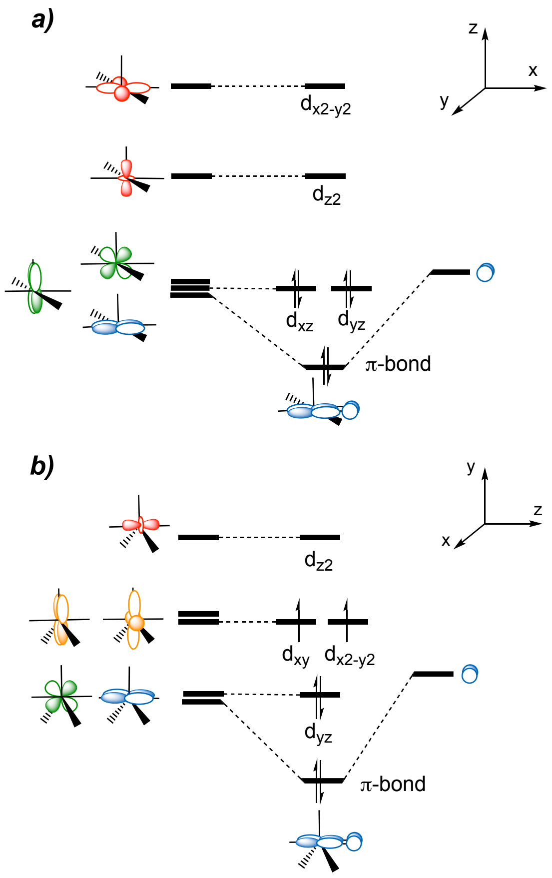

Figure 1. Schematic Molecular Orbitals diagram of ideal SBP(a) and TBP (b) d^6 complexes.

The triplet state structures of **1**, **2** and **4** also present a distorted SBP coordination around the metal center (Figures S1 to S6 of the ESI). In contrast, complexes **3**, **3_H** and **5** are characterized by a trigonal bipyramid (TBP) geometry. This can be, at least, partially explained analyzing the molecular orbital diagrams of ideal SBP and TBP d^6 metal complexes. It was mentioned above that the low-spin state of an ideal d^6 complex with a SBP coordination around the metal center corresponds to a singlet state. However, if the splitting between the d_{xz} or d_{yz} and the d_{z2} orbitals (Figure 1a) is small, the situation in which one electron of either the d_{xz} or the d_{yz} orbital occupies the d_{z2} orbital becomes energetically accessible. On the other hand, an ideal TBP complex shows two degenerate orbitals (d_{xy} and d_{x2-y2}) that should be singly occupied in a d^6 electronic configuration, thus resulting also in a triplet state (Figures 1b and S11). The preference for one or other situation may depend on the constraints arising from the chelating ligand as well as on the σ-donating ability of the ancillary ligands.

Regardless of the coordination around the metal center, in all triplet states, the $Fe=CH_2$ bond distance is larger than that of the singlet (between 1.749 and 1.792 Å) and the carbene substituents are not fully perpendicular to the plane in which the π-bond is formed. These two facts are associated with a spin distribution suggesting a situation in between a formed $Fe=CH_2$ double bond with two unpaired electrons on the metal center and a situation in which the π bond of $Fe=CH_2$ is not formed and thus three unpaired electrons are located over the metal center and one (with the opposite spin) on the carbene carbon (see Figure S11 for a schematic representation of the two limit situations). It is worth mentioning that this latter configuration has already been described for the triplet ground state of the (^{R}PDI)$Fe=CPh_2$ (PDI = bis(imido)pyridine) complex synthetized by Chirik and co-workers.[41] Overall, the larger $Fe=CH_2$ distance and the spin density distribution are indicative of a significantly weaker π-bond in the triplet state and this is also highlighted by the smaller Wiberg bond index and delocalization predicted by AIM (Table S2). In the case of the quintet states, the $Fe=CH_2$ bonds are even longer and the spin distribution suggests a larger radical character on the carbene, thereby indicating that the π bond is even weaker in the S = 2 state.

Regarding the energetics (Table 1), complexes **1**, **2** and **5** which mainly have neutral N-based ligands except the carbene, present a triplet ground state. In contrast, complexes **3**, **3_H** and **4**, with either three strong donating N-Heterocyclic carbene (NHC) ligands or one C-based anionic group, present a singlet ground state. This difference between the two sets of complexes can be explained by the effect of σ-donating ligands that stabilizes the low spin state. Remarkably, the relative stabilities of the three spin states are very similar for complexes **3** and **3$_H$** suggesting that the phenyl groups have a small influence on the spin multiplicity of the ground state.

At this point it is worth mentioning that an isomer in which the carbene inserts in either the Fe-N bond involving the pyridine ligand, the Fe-C bond of the N-heterocyclic carbene or the Fe-C bond involving the phenyl ligand of **4** is found to be a minimum of the potential energy surface too. The resulting species, hereafter referred to as bridged carbenes, resemble the ones recently reported as a masked carbene complex (See Figure S12 of the ESI).[27] The bridged carbenes of complexes **1** to **5** present a quintet ground state (see Table S3) and they are usually more stable than the normal carbene. This suggests that their formation should be prevented, in order to obtain a singlet state carbene.

Regardless of the electronic state, all stable metallacyclobutanes resulting from the reaction of the methylidenes **1** to **5** with ethene present an octahedral coordination around the metal center.[72] The analysis of the spin densities suggests that, in all cases, the unpaired electrons are localised on the metal atom. Significant differences in the geometrical features of the metallacyclobutane fragment are observed as a function of the spin state. Singlet state metallacyclobutanes are characterized by relatively short M-C$_\alpha$ distances, relatively large C$_\alpha$-C$_\beta$ bonds and relatively large C$_\alpha$-C$_\beta$-C$_\alpha$ angles. This three structural changes make the M-C$_\beta$ distances shorter, as already described for the d^0 and Ru-based TBP metallacyclobutanes involved in alkene metathesis.[73–77] In contrast, triplet metallacyclobutanes present larger M-C$_\alpha$ distances, shorter C$_\alpha$-C$_\beta$ bonds and M-C$_\beta$ distances that are at least 0.3 Å longer than those of the singlet state intermediates (Figures S1 to S6). Overall, the open shell metallacycles are geometrically closer to those of the d^0 SBP metallacyclobutane that do not perform metathesis.[73–75] However, these geometrical differences of the metallacycle do not arise from a change on the coordination around the metal center as it is the case for the pentacoordinated metallacyclobutanes, but from a different occupation of the metal d orbitals. The importance of the metal d orbital occupation is schematically represented in Figure 2, which shows (a) an ideal molecular orbital diagram for a d^4 octahedral metal complex (iron is formally Fe(IV) in the metallacycle) and (b) the associated natural orbitals (NO) of the triplet state of **1**. The d_{xz} orbital in the triplet state metallacycles is singly occupied and points towards the $C_{\beta,}$. This produces a repulsive interaction of such orbital with a doubly occupied orbital of the metallacyclobutane fragment that is minimized by pushing the C_{β} away from the metal center. In contrast, the d_{xz} orbital is empty in the singlet state and thus, there is no repulsion with the occupied orbitals centered on metallacyclobutane fragment and the C_{β} can be found closer to the metal atom. Overall, as already found for $L_3Fe{=}CH_2$ species,[44] the $Fe(CH_2CH_2CH_2)$ geometrical features suggest that singlet state metallacyclobutanes are more prone to undergo metathesis than the triplet state ones.

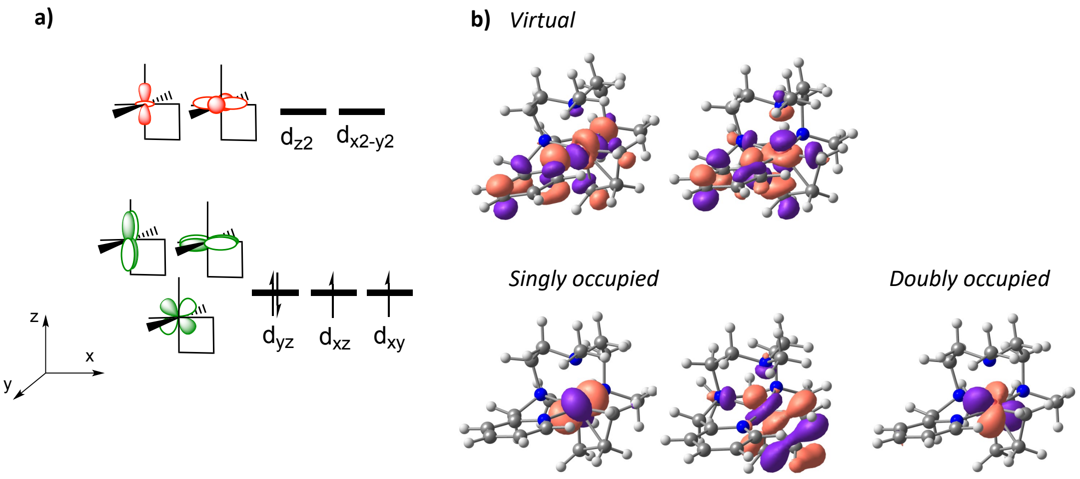

Figure 2. (a) Schematic Molecular Orbitals diagram for an ideal high field d^4 octahedral metallacyclobutane intermediate. (b) The associated Natural Orbitals of the metallacyclobutane S = 1 state arising from the reaction of **1** with ethane.

The metallacyclobutane formation from the reaction between the methylidene and ethene is favorable for all singlet and triplet states, except for the case of **3**, where the presence of the phenyl substituents prevents the olefin coordination. Indeed, while the substitution of the Ph group by H atoms has little influence on the relative stabilities of the different spin states, it dramatically modifies the tendency to react with an incoming olefin (compare **3** with **3**$_{\mathbf{H}}$ in Table 1). Moreover, the addition of C-based ligands leads also to less stable metallacyclobutanes. However, in this case, this seems to be appropriate because, while values for **1**, **2** and **5** appear too negative for an efficient catalytic process, the ones for **3$_H$** and **4** are closer to the values computed with the same methodology for the efficient 2nd generation Grubbs catalyst (**0**).[44,77] Unfortunately, the metallacyclobutane intermediate generally presents a triplet ground state, a spin state that it is less prone to undergo metathesis. The unique exception, in the initial set of complexes, is **4**. Note that iron is formally Fe(IV) in the metallacycle intermediate and thus, $S = 1$ is the preferred spin state for an ideal low spin octahedral complex (see Figure 2). However, the ligands of **4** present significantly different σ-donating abilities. This breaks the degeneracy of the t_{2g} orbitals, the splitting between them being large enough to favor a singlet ground state.

Finally, alkane cyclopropanation (the reported values for the cyclopropanation reaction correspond to the Gibbs energy difference between the cyclopropanation products and the carbene + ethene) is highly favorable for complexes **1** to **5** in all spin states. The reaction ΔG°_{298K} ranges from -50.8 to -13.9 kcal mol^{-1}. This shows that these complexes are not suitable candidates for alkene metathesis. Complexes **3$_H$** and **4** present the least favorable cyclopropanation reaction energy, which is consistent with the presence of stronger σ-donor ligands. Indeed, the Fe=CH$_2$ bond in the singlet state is stronger for complexes **3$_H$** and **4** than for the other species of this set (See Table 2) and the energetics for cyclopropanation is found to be less favorable. The resulting metal fragment has a butterfly coordination around the metal center in most singlet and triplet states, whereas it presents a trigonal pyramid structure in the quintet states with flexible ligands. Regardless of the coordination around the metal center, the quintet ground state presents four unpaired electrons that, as in the case of the triplet state, are localized on the metal center. By comparing the energetics of **3** and **3$_H$** it can be deduced that the presence of the phenyl groups makes the alkene cyclopropanation more favorable and thus, overall, **3$_H$** appears to be the best candidate for further modifications.

Overall, complexes **1** to **5** do not appear to be good candidates for alkene metathesis. Three main drawbacks can be identified: i) the singlet state is usually not the ground state for the metal carbene;

ii) the metallacyclobutane intermediate generally presents a triplet ground state and iii) the alkene cyclopropanation is largely favored with respect to the alkene metathesis reaction. The addition of C-based ligands appears to stabilize the singlet state carbene, destabilize the metallacyclobutane intermediate and, makes the alkene cyclopropanation less favorable. Thus, complexes with σ-donating ligands seem to be good candidates that should be further analyzed. However, before that the flexibility of the chelating ligands has been analyzed.

Table 2. Fe=CH_2 binding energies (kcal mol^{-1}). The binding energy corresponds to the energy difference between the metal-carbene in the singlet state and the [M] and CH_2 neutral triplet state fragments.

Complex	BDE	**Species**	BDE	**Species**	BDE	**Complex**	BDE	**Complex**	BDE
0	-88.1	$\mathbf{1_{322}}$	-57.1	$\mathbf{1_{Pyreq}}$	-65.3	$\mathbf{5_{CeqCtrans}}$	-58.7	$\mathbf{4_{CeqOtrans}}$	-86.1
1	-66.3	$\mathbf{1_{232}}$	-53.9	$\mathbf{1_{Pyrap}}$	-56.0	$\mathbf{5_{CapCtrans}}$	-65.3	$\mathbf{1_{0}}$	-80.5
2	-61.2	$\mathbf{1_{223}}$	-63.5	$\mathbf{1_{Pyrtrans}}$	-52.8	$\mathbf{2_{CapCtrans}}$	-71.6	$\mathbf{2_{0}}$	-67.7
3	-65.0	$\mathbf{1_{332}}$	-47.7	$\mathbf{1_{CeqCap}}$	-77.9	$\mathbf{3_{H\text{-}Ctrans}}$	-65.9	$\mathbf{3_{0}}$	-81.0
$\mathbf{3_{H}}$	-73.1	$\mathbf{1_{323}}$	-48.7	$\mathbf{1_{CeqCtrans}}$	-54.5	$\mathbf{4_{Ctrans}}$	-79.7	$\mathbf{5_{0}}$	-84.1
4	-81.4	$\mathbf{1_{233}}$	-51.0	$\mathbf{1_{CapCtrans}}$	-74.7	$\mathbf{4_{Otrans}}$	-78.8		
5	-69.5	$\mathbf{1_{333}}$	-46.0	$\mathbf{5_{CeqCap}}$	-78.4	$\mathbf{4_{PeqOtrans}}$	-78.1		

Chelating ligand flexibility. The complexes designed *in-silico* for exploring the effect of the chelating ligand flexibility, are depicted in Scheme 3. They are all based on the complex **1** in which, either the length of the alkyl chains between N based groups have been increased from ethyl to propyl, or one of the amine ligands has been replaced by a pyridine molecule. This latter modification implies both a change on the rigidity of the chelating ligand (pyridine can be linked to a maximum of two other ligands, whereas the amine can be linked to three) and on the σ- and π-donating ability of the ligands. By comparing the results for the complexes $\mathbf{1_{Peq}}$, $\mathbf{1_{Pap}}$, $\mathbf{1_{Ptrans}}$ and **2,** it is possible to understand how the different connectivity and the pyridine position and orientation, influences the stabilities of the different spin states and the thermodynamics for alkene metathesis and alkene cyclopropanation. Results are shown in Table 2, where the coordination around the metal center in the carbene together with all the energetics associated to the carbene, metallacyclobutane intermediate and cyclopropanation products are reported. The Cartesian coordinates of all optimized structures can be found in the ESI.

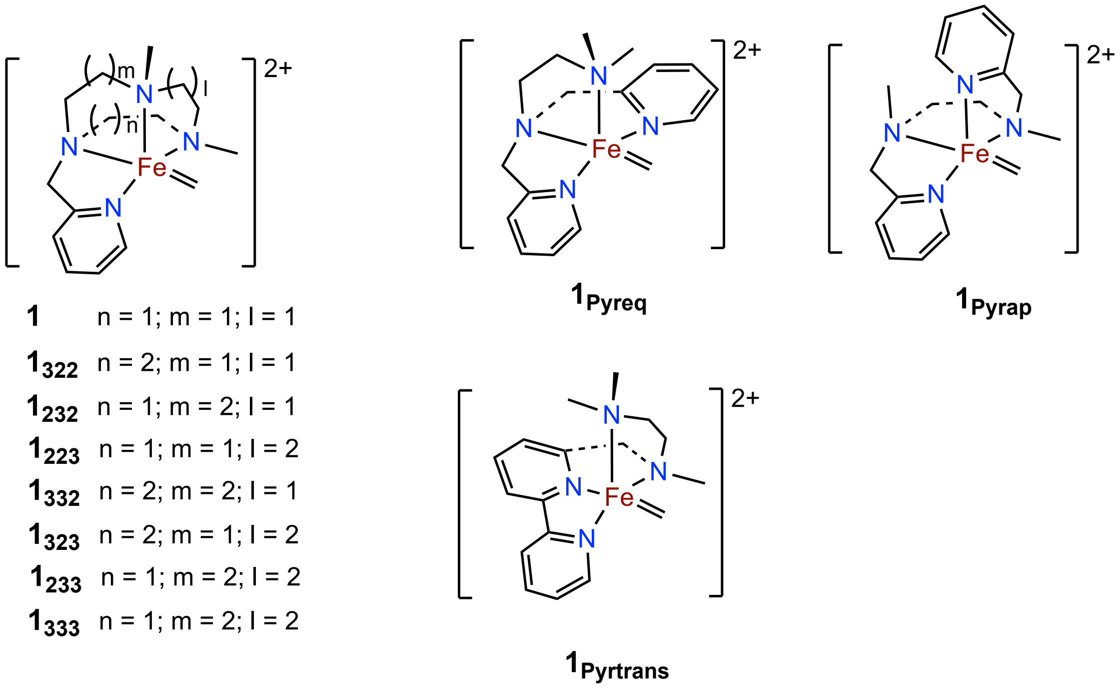

1 n = 1; m = 1; l = 1

$\mathbf{1_{322}}$ n = 2; m = 1; l = 1

$\mathbf{1_{232}}$ n = 1; m = 2; l = 1

$\mathbf{1_{223}}$ n = 1; m = 1; l = 2

$\mathbf{1_{332}}$ n = 2; m = 2; l = 1

$\mathbf{1_{323}}$ n = 2; m = 1; l = 2

$\mathbf{1_{233}}$ n = 1; m = 2; l = 2

$\mathbf{1_{333}}$ n = 1; m = 2; l = 2

$\mathbf{1_{Pyreq}}$

$\mathbf{1_{Pyrap}}$

$\mathbf{1_{Pyrtrans}}$

Scheme 3.

From these results, it can be observed that a change in the length of the alkyl chain between the N-based ligands and the number of amine and pyridine groups has little influence on the geometries around the metal center of the species discussed in this subsection, the most significant ones being found for the carbene and the metal fragment resulting from the cyclopropanation. With respect to the metal fragment resulting from the alkene cyclopropanation, the presence of flexible ligands leads to a larger variety of coordination geometries around the metal center, the most common ones being the butterfly and the trigonal pyramid structures. Regarding the carbene, all singlet state carbenes present a square based pyramid (SBP) coordination around the metal center as in the case of complexes **1** to **5**. However, the larger flexibility of the chelating ligand seems to make angles larger than 90^{o} more favorable and thus, the majority of the triplet and quintet states present a trigonal bipyramid structure (TBP). These two geometries are consistent with the low spin state of the molecular orbital diagrams shown in Figure 1. Therefore, the final geometry of the triplet state seems to be at least in a large extend controlled by the constraints imposed by the flexibility of the chelating ligand. It is also worth mentioning that the Fe=CH_2 bond dissociation are lower than that of **1** and this effect is more pronounced for complexes having several propyl chains between N-based ligands.

Table 3. Relative Gibbs (G_{gp} + D2) energies of the species involved in the metathesis and cyclopropanation reactions of iron carbene complexes $\mathbf{1}_{nml}$ and $\mathbf{1}_{Pyr}$ with respect to the carbene singlet state and ethene. All values are in kcal mol^{-1}.

Complex	**Geometry**[a]			**Carbene**			**Metallacyclobutane**			**Cyclopropanation**		
	S=0	***S=1***	***S=2***	***S=0***	***S=1***	***S=2***	***S=0***	***S=1***	***S=2***	***S=0***	***S=1***	***S=2***
$\mathbf{1}_{322}$	SBP	--[c]	--[c]	0.0	-9.8	0.0	-19.3	-23.6	--[d]	-31.2	-38.9	-53.4
$\mathbf{1}_{232}$	SBP	--[c]	TBP	0.0	-7.0	-3.4	-10.3	-19.9	--[d]	-27.3	-40.3	-54.5
$\mathbf{1}_{223}$	SBP	TBP	TBP	0.0	-11.1	6.2	-6.8	-21.5	--[d]	-25.7	-31.8	-51.4
$\mathbf{1}_{332}$	SBP	SBP	TBP	0.0	-11.7	-5.6	-13.3	-24.9	--[d]	-31.4	-47.5	-64.5
$\mathbf{1}_{323}$	SBP	TBP	TBP	0.0	-12.6	-1.9	-19.7	-48.8	--[d]	-36.0	-47.2	-58.9
$\mathbf{1}_{233}$	SBP	TBP	TBP	0.0	-10.9	-4.6	N.A.	N.A.	--[d]	-28.5	-42.8	-61.6
$\mathbf{1}_{333}$	SBP	TBP	TBP	0.0	-16.5	-7.0	-10.7	-23.6	--[d]	-37.8	-49.4	-71.9
$\mathbf{1}_{Pyreq}$	SBP	TBP	TBP	0.0	-12.3	-2.6	-23.8	-27.3	--[d]	-23.7	-30.4	-52.7
$\mathbf{1}_{Pyrap}$	SBP	--[c]	TBP	0.0	-7.7	2.0	-13.1	-18.5	--[d]	-24.5	-39.2	-52.2
$\mathbf{1}_{Pyrtrans}$	SBP	--[c]	TBP	0.0	-6.3	-6.0	N.A.	-23.3	--[d]	-26.5	-47.0	-48.2

[a] Coordination around the metal center in the carbene.

[b] The cyclopropanation values correspond to the Gibbs energy difference between cyclopropanation products and the initial carbene + ethene.

[c] Coordination in between the SBP and TBP.

[d] Geometry spontaneously evolved towards the formation of cyclopropane upon optimization.

Regarding the energetics, it can be observed that: i) all the $\mathbf{1}_{nml}$ and $\mathbf{1}_{Pyr}$ carbenes present a triplet ground state, which lies between -6.3 and -16.5 kcal mol^{-1} below the singlet state; ii) the metallacyclobutane has also a triplet ground state whose formation is exergonic with respect to the isolated reactants and iii) the alkene cyclopropanation reaction is extremely favorable, the reaction Gibbs energies ranging from -23.7 and -71.9 kcal mol^{-1}. These general trends are equivalent to those found for complexes **1** and **2** and suggest that modifications on the ligand flexibility are not sufficient to overcome the drawbacks found for the first set of complexes. However, the increased flexibility of the ligands has several consequences. For example, the singlet state carbenes present a SBP geometry with angles between ligands of 90° and most of the triplets have TBP structures which require angles of 120°. Therefore, increasing the length of the alkyl chain between N groups or increasing the flexibility of the ligand, by replacing one amine group with a pyridine, stabilizes the triplet state. As a matter of fact, the triplet state becomes more stable for the $\mathbf{1}_{\mathbf{nml}}$ and $\mathbf{1}_{\mathbf{Pyr}}$ complexes than for complex **1**. Similarly, the formation of the octahedral metallacyclobutane, which is characterized by the presence of angles of 90° between the ligands too, is marginally destabilized in the singlet state when using chelating ligands with larger chain between the donating groups. Finally, the alkene cyclopropanation becomes even more favorable when the length of the alkyl chain is increased. Overall, these trends suggest that rigid chelating ligands may stabilize the carbene singlet state and make the alkene cyclopropanation less favorable. Consequently, complexes **1** to **5** appear more appropriate than the $\mathbf{1}_{\mathbf{nml}}$ and $\mathbf{1}_{\mathbf{Pyr}}$ derivatives for further studies of the effect induced by changing the σ-donating ability of the ligands on the initial metal carbeness.

Effect of the σ-donating ability of the ligands. The results for the initial set of complexes shows that the σ-donating ability of the ancillary ligands has an important influence on the multiplicity of spin of the ground state and on the thermodynamics of the cyclopropanation reaction. Therefore, we decided to further analyze the consequences of modifying the σ–donating ability of the ancillary ligands. In this context, we adopted two different strategies. First, we considered the complexes of the initial set and we substituted one or two N-based neutral ligands with alkyl groups, the number of substitutions was determined in order to obtain a neutral compound. We chose alkyl ligands as they have a significantly stronger donor character than the amines, although they could potentially be involved in undesired side reactions, which are not considered here. We considered $\mathbf{3}_{\mathbf{H\text{-}C}}$ and not $\mathbf{3}_{\mathbf{C}}$ (where the N-substituents are H atoms instead of phenyl groups) because $\mathbf{3}_{\mathbf{H}}$ is more reactive towards olefins. In addition, we explored the possibility of decreasing the σ-donating ability of the group *trans* to the carbene by substituting the N-based ligand with an ether group. We considered only derivates of the complex **4** as this one is the only one of the initial set presenting a singlet ground state for the carbene and the metallacyclobutane. The resulting set of complexes are shown in Scheme 4, the associated energetics are reported in Table 3 and the Cartesian coordinates of the optimized structures are given in the ESI.

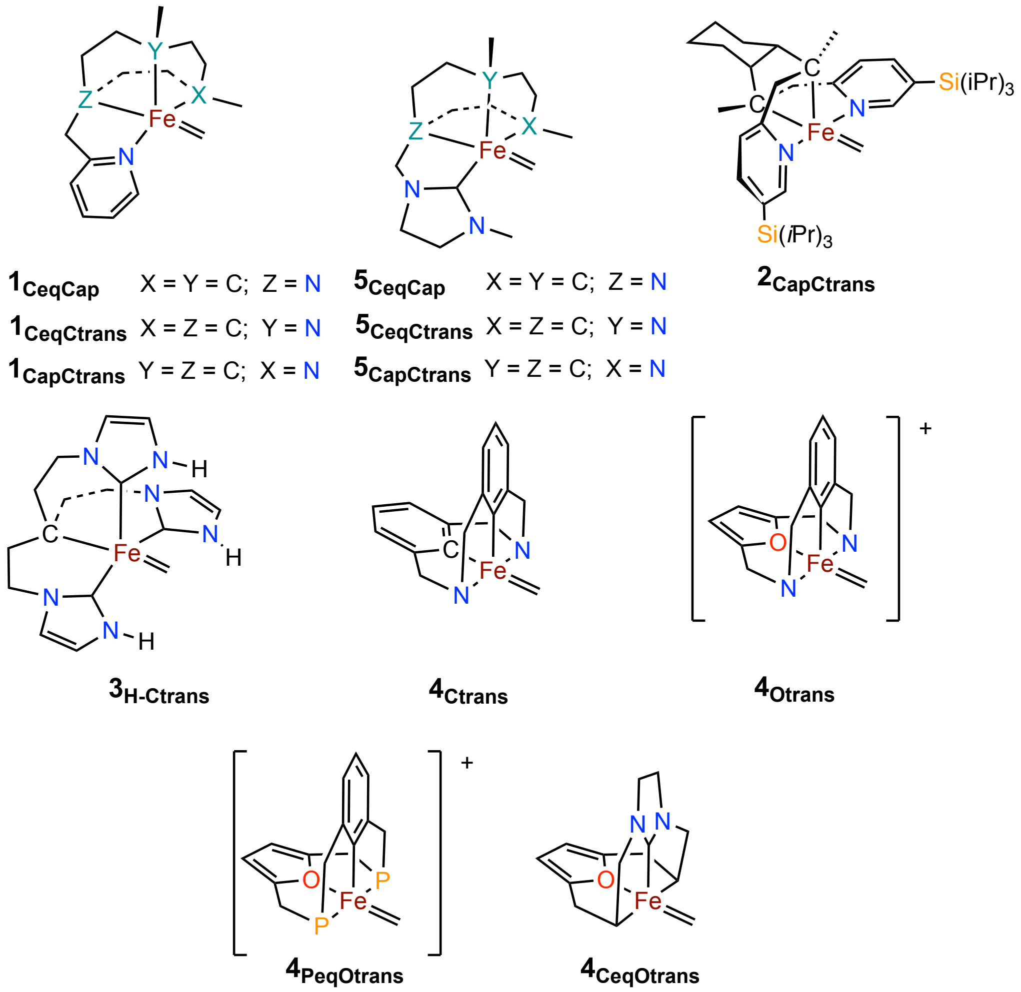

Scheme 4.

The substitution of N-based neutral ligands with alkyls has little influence on the geometry around the metal center of the carbene, on the metallacyclobutane and on the fragments arising from the cyclopropanation reaction. As a matter of fact, the most remarkable change is the presence of two singlet state species ($\mathbf{1}_{\mathrm{CapCtrans}}$ and $\mathbf{2}_{\mathrm{CapCtrans}}$) where the coordination around the metal center is unexpectedly a trigonal bipyramid. Besides, the Fe=CH$_2$ bond becomes stronger when adding σ-donor groups *cis* to the carbene. Remarkably, the opposite trend is observed when the alkyl group is added *trans* to the carbene (Table 2).

Table 4. Relative Gibbs (G_{gp} + D2) energies of the species involved in the metathesis and cyclopropanation reactions iron carbene complexes resulting from the substitution of N-based ligands by either C-based or O-based ones with respect to the carbene in its singlet state and the ethene. All values are in kcal mol^{-1}

Complex	Geometry[a]			Carbene			Metallacyclobutane			Cyclopropanation[b]		
	S=0	*S=1*	*S=2*	*S=0*	*S=1*	*S=2*	*S=0*	*S=1*	*S=2*	*S=0*	*S=1*	*S=2*
1$_{\text{CeqCap}}$	SBP	SBP	TBP	0.0	3.2	16.1	-7.1	-13.8	2.3	-11.6	-19.0	-21.4
1$_{\text{CeqCtrans}}$	SBP	SBP	--[c]	0.0	-12.3	-1.8	-20.1	-28.4	N.A	-30.7	-40.3	-34.1
1$_{\text{CapCtrans}}$	TBP	TBP	TBP	0.0	9.8	17.6	-3.7	N.A	N.A	-23.8	-21.8	-18.3
5$_{\text{CeqCap}}$	SBP	SBP	--[c]	0.0	9.1	21.9	5.3	-2.7	12.4	-9.3	-17.5	-16.7
5$_{\text{CeqCtrans}}$	SBP	--[c]	TBP	0.0	-9.1	4.2	N.A	-21.6	0.3	-26.1	-37.0	-29.9
5$_{\text{CapCtrans}}$	SBP	TBP	TBP	0.0	-0.9	13.3	--[e]	-8.5	5.6	-29.0	-29.4	-23.0
2$_{\text{CapCtrans}}$	TBP	TBP	TBP	0.0	11.8	23.3	-2.6	-1.3	3.7	-26.2	-21.9	-19.8
3$_{\text{H-Ctrans}}$	SBP	TBP	TBP	0.0	5.3	20.1	-8.9	-8.0	24.4	-36.2	-29.0	-29.4
4$_{\text{Ctrans}}$	SBP	TBP	TBP	0.0	5.1	7.0	-15.4	-11.2	-12.0	-25.3	-16.3	-16.4
4$_{\text{Otrans}}$	SBP	--[c]	--[c]	0.0	9.2	7.0	-7.8	-7.4	-12.5	-2.8	-19.0	-22.1
4$_{\text{PeqOtrans}}$	SBP	SBP	--[d]	0.0	5.6	--[d]	-13.0	-10.2	1.5	-1.9	-19.5	-13.9
4$_{\text{CeqOtrans}}$	SBP	SBP	TBP	0.0	13.0	31.2	-3.7	-5.3	13.0	11.8	-12.5	-1.7

[a] Coordination around the metal center in the carbene.

[b] The cyclopropanation values correspond to the Gibbs energy difference between cyclopropanation products and initial carbene + ethene.

[c] Coordination in between the SBP and TBP.

[d] The Fe=CH_2 carbene is not a minimum of the potential energy surface, optimization leads to carbene insertion into the C-based ligand .

[e] Geometry spontaneously evolved towards the formation of cyclopropane upon optimization.

As observed for the first set (**1** to **5**), the addition of C-based ligands generally stabilizes the singlet state, destabilizes the metallacyclobutane intermediate and makes alkene cyclopropanation slightly less favorable (Table 4). The latter can be associated with a Fe=CH_2 bond strengthening. However, there are several exceptions to this general behavior. In this way, the ligands present in complexes **1**$_{\text{CeqCtrans}}$, **1**$_{\text{CapCtrans}}$, **5**$_{\text{CeqCtrans}}$, **5**$_{\text{CapCtrans}}$, **3**$_{\text{H-C}}$ and **4**$_{\text{Ctrans}}$ make the carbene singlet state less stable and the cyclopropanation becomes even more favorable than their related compounds bearing N-based ligands (**1**, **3**$_{\text{H}}$, **4** and **5**). This is related to the fact that the N to C substitution is performed *trans* to the carbene, which generally weakens the Fe=CH_2 bond despite the increased electron density on the metal. This data suggests that the strong donating groups should be *cis* to the carbene, indicating that, as already found for $L_3Fe=CH_2$ complexes,[78] there are preferred positions for the σ-donating groups if one wants to prevent the alkene cyclopropanation. Overall, most of the complex of this series present the desirable singlet ground state, but unfortunately, several drawbacks persist. In this view, although the preference for cyclopropanation is reduced, this process is still usually largely more favorable than metathesis in all spin states. In addition, results suggest that the metallacyclobutane intermediate has a triplet ground state in most of the cases. In fact, for complexes **2**$_{\mathbf{CapCtrans}}$**,** **3**$_{\mathbf{H\text{-}Ctrans}}$ and **4**$_{\mathbf{Ctrans}}$, the singlet state is more stable than the triplet but only for the last one the energy difference is significant (4.2 kcal mol^{-1}). In fact, as mentioned above, one would expect a triplet ground state in all cases as it is the ideal situation for a d^4 low spin octahedral complex (Figure 2). Therefore, the stabilization of the singlet state can only be understood as a significant destabilization of the iron d orbital pointing toward the C$_\beta$ of the metallacycle. In this context, only when this destabilization is large enough, the ground state becomes a singlet and this could eventually be a potential strategy to make the metallacyclobutane singlet state more favorable.

With the aim of further confirming that the presence of a strong donating ligand *trans* to the carbene is detrimental to the achievement of a singlet ground state for the carbene and for making the alkene cyclopropanation reaction less favorable, we considered three additional complexes deriving from **4**. These three complexes present a furane ligand instead of the pyridine *trans* to the carbene and they differ by the other ligands in the basal plane of the SBP carbene structure (amines *vs.* phosphines or alkyls). The corresponding energetics show that the O by N substitution has little influence on the relative stabilities of the different spin states of the carbene and the metallacyclobutane, but strongly undermines the alkene cyclopropanation. This is associated with the strengthening of the Fe=CH$_2$ bond. Indeed, complexes **4**$_{\mathbf{Otrans}}$, and **4**$_{\mathbf{PeqOtrans}}$ show a singlet ground state for the metal carbene and the metallacyclobutane intermediate, and cyclopropanation in the singlet state is not particularly more favorable thermodynamically than metathesis. Similarly, complex **4**$_{\mathbf{CeqOtrans}}$ presents a singlet ground state carbene and a non-favorable alkene cyclopropanation in the singlet state. However, in this latter case, the metallacyclobutane has a triplet ground state, the singlet being 1.6 kcal mol^{-1} higher in energy. Overall, complexes **4**$_{\mathbf{Otrans}}$, **4**$_{\mathbf{PeqOtrans}}$ and **4**$_{\mathbf{CeqOtrans}}$ can be considered as the first three species reported here that show similar thermodynamics to those of the Ru-based reference system **0**.

Influence of metal reduction. Finally, we expected that metal reduction leading to formally Fe(0) carbenes[79] could stabilize singlet state metallacyclobutanes. This assumption arises from the fact that this intermediate would present a formal Fe(II) metal center with formally six d electrons in an octahedral environment. In this way, the singlet state would be the ground state of the low spin structure and this would not depend on the splitting between the ideal t_{2g} orbitals. Furthermore, the additional electrons could reinforce the Fe=CH_2 bond and thus, make alkene cyclopropanation less favorable. We analyzed this hypothesis by reducing the metal center of the doubly positively charged complexes **1**, **2**, **3_H** and **5**, the resulting complexes **1_0, 2_0, $3_{H\text{-}0}$ and 5_0** being globally neutral (Scheme 2). Table 5 lists the associated energetics and the optimized geometries can be found in the ESI (Figures S7 to S10).

Results show that the reduction of the metal center on complexes **8** to **11** implies important geometrical rearrangements in the carbene and in the metallacycle (Figures S7 to S10 of the ESI). Regarding the carbene, the formally Fe(II) complexes generally present a SBP coordination in the singlet state but, the reduced species present a TBP one. This is accompanied by an elongation of the Fe=CH_2 bond, which becomes around 1.76 Å. All triplet state carbenes present a SBP geometry around the metal center. The changes in the coordination geometry around the metal can be rationalized by the increased number of d electrons of iron. Low spin pentacoordinated d^8 complexes are expected to be TBP (see Figure 1). The metallacyclobutane intermediate presents the expected octahedral coordination around the metal center, but the large C_α-C_β-C_α angle and the short M···C_β distance typically found in metallacyclobutanes involved in metathesis is not observed in any of the spin states. This can be attributed again to the two additional d electrons of iron that in the case of the singlet state occupy the d orbital pointing towards C_β (Figure 2).

The thermodynamics of the formally Fe(0) complexes is substantially different from that of the formally Fe(II) complexes. First, in contrast to what is obtained for the analogous Fe(II) **1**, **2** and **5** complexes, the reduced species present generally a singlet ground state. Moreover, the formation of the metallacyclobutane is exergonic and leads to intermediates with the desirable singlet state. Finally, alkene cyclopropanation becomes unfavorable in the singlet state and, although it remains exergonic for the triplet and most of the quintet states, the obtained values are closer to those computed for the second generation Grubbs catalyst (**0**). This is particularly noticeable in the case of $\mathbf{5_0}$, which is an *in-silico* modification of the ligands used by Costas and co-workers for the synthesis of iron oxo complexes. Overall, from a thermodynamic point of view the reduced complexes appear to be promising candidates, $\mathbf{5_0}$ being the most interesting one.

Table 5. Relative Gibbs (G_{gp} + D2) energies of the species involved in the metathesis and cyclopropanation reactions of iron carbene complexes $\mathbf{1_0}$ **to** $\mathbf{5_0}$ with respect to the carbene singlet state and ethene. All values are in kcal mol^{-1}

Complex	**Geometry**[a]			**Carbene**			**Metallacyclobutane**			**Cyclopropanation**[b]		
	S=0	***S=1***	***S=2***	***S=0***	***S=1***	***S=2***	***S=0***	***S=1***	***S=2***	***S=0***	***S=1***	***S=2***
$\mathbf{1_0}$	TBP	SBP	SBP	0.0	-0.4	0,2	-26.5	-21.9	-18.9	4.8	-17.1	-12.9
$\mathbf{2_0}$	TBP	SBP	SBP	0.0	2.9	12.3	-15.1	-12.3	--[e]	4.9	-29.7	-21.7
$\mathbf{3_0}$	TBP	SBP	--[d]	0.0	9.3	--[d]	-23.4	-0.9	23.3	-0.6	-16.6	0.9
$\mathbf{5_0}$	TBP	--[c]	SBP	0.0	4.9	7,6	-23.3	-12.4	-10.2	8.9	-12.2	-3.1

[a] Coordination around the metal center in the carbene.

[b] The cyclopropanation values correspond to the Gibbs free energy difference between cyclopropanation products and carbene + ethene.

[c] Coordination in between the SBP and TBP.

[d] The Fe=CH_2 carbene is not a minimum of the potential energy surface, optimization leads to carbene insertion into the C-based ligand

[e] Geometry spontaneously evolved towards the formation of cyclopropane upon optimization.

Energy barriers for selected carbenes. As mentioned above, the Fe(II) complexes $\mathbf{4_{Otrans}}$ $\mathbf{4_{PeqOtrans}}$, $\mathbf{4_{CeqOtrans}}$ and the reduced Fe(0) species $\mathbf{1_0}$, $\mathbf{2_0}$ and $\mathbf{5_0}$ appear as potentially promising candidates, since their thermodynamic properties resemble that of the second generation Grubbs catalysts. Therefore, we decided to explore the energetics of the transition states associated with the cycloreversion and other deactivation processes (mainly cyclopropanation) for one selected case of each set ($\mathbf{4_{CeqOtrans}}$ and $\mathbf{5_0}$). In the case of the deactivation process of $\mathbf{5_0}$, two pathways have been explored: the carbene extraction by ethene that mainly leads to cyclopropanation through a stepwise (CP-SW) process and the cyclopropanation from metallacyclobutane intermediate (CP-MC). Besides, while we have only considered the singlet state in the alkene metathesis cycloreversion process, we explored both the singlet and triplet states in the deactivation pathways. In the case of cyclopropanation, a spin crossing is expected as reactants have a singlet ground state, whereas cyclopropanation products have a triplet one. For comparison purposes, we also considered the complex **5**, which is the oxidized analogue of **5**$_0$. The Gibbs energy profile associated with the reactivity of **4**$_{CeqOtrans}$ with ethene is reported in Figure 3. Results for **5**$_0$ can be found in Figure 4 where the transition states of the alkene metathesis cycloreversion process are reported. The Gibbs energy profile for the reactions involving **5**$_0$ are reported in Figure 5. Finally, results for **5** are reported in the ESI.

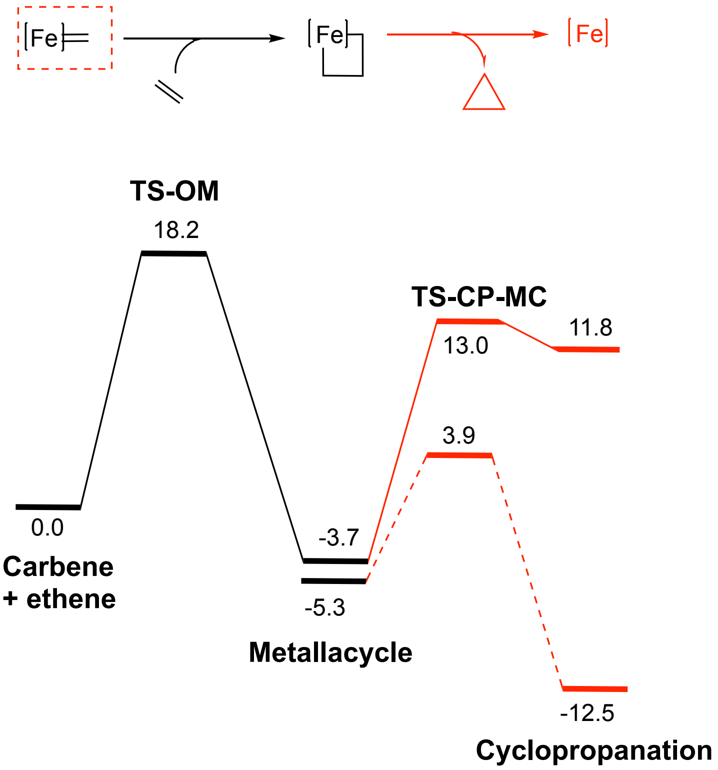

Figure 3. Gibbs energy profile (in kcal mol^{-1}) for the reaction of **4**$_{CeqOtrans}$ with ethene. Black lines correspond to the alkene metathesis cycloreversion step while red lines correspond to the alkene cyclopropanation involving the metallacyclobutane intermediate. Solid lines are used for the singlet (S=0) state and dashed ones for the triplet (S=1) state.

Alkene metathesis involving **4**$_{CeqOtrans}$ takes place through the classical cycloaddition and cycloreversion steps. Cycloreversion presents the highest transition state which is 18.2 kcal mol^{-1} higher in energy than the separated reactants. This leads to a Gibbs energy barrier from the more stable metallacylobutane of 21.9 kcal mol^{-1}, which is moderate but still higher than the traditional values for cycloaddition and cycloreversion.[80–88] The energy barriers for cyclopropanation from the metallacyclobutane are significantly lower, both in the singlet and triplet state, suggesting that the complex $\mathbf{4}_{\mathbf{CeqOtrans}}$ would be more prone to undergo cyclopropanation. Remarkably, the moderate energy barrier obtained for the cycloreversion process can be associated with the weak σ-donating ability of the furane ligand, which is in *trans* to the olefin that is being released.[89–91] However, this ligand is mandatory since it makes the cyclopropanation thermodynamically unfavorable, thus it combines both beneficial and detrimental effects. As a consequence, only a subtle balance of the two effects could lead to species with a kinetic preference for alkene metathesis. Alternatively, a labile ligand could decoordinate during the cycloaddition and cycloreversion step leading to a tetracoordinated system with larger flexibility to help both in the coordination of the olefin and its release *trans* to an strong donating ligand. [80–88]

Regarding $\mathbf{5}_0$, the metallacyclobutane formation from separated reactants (methylidene + ethene) takes place in two steps. These two steps correspond to: i) the formation of the Fe-C between one carbon of the olefin and the metal center and ii) the formation of the C-C bond coupling between the carbene and the other end of the olefin. These two steps are completely different from those reported for the usual alkene metathesis reaction catalyzed by the Mo, W or Ru complexes (alkene coordination and cycloaddition)[73,74,80,81,88,82–87] and this can be rationalized by formal electron counting (see below). In addition, the intermediate resulting from the formation of the Fe-C bond formation is largely unstable, its energy is 26.3 kcal mol^{-1} higher than the separated reactants and it presents Fe···N distances that have been largely elongated. One of these Fe···N distance is so large (> 3.4 Å) that indicates a decoordination of the ligand. The release of the olefin from the metallacycle takes place in equivalent steps, although the geometries and energetics are slightly different, since the two processes take place with two different ligands in *trans*. The associated energetics suggest that alkene metathesis with $\mathbf{5}_0$ is kinetically unfavorable. The highest energy barrier associated to the cycloaddition is 35.7 kcal mol^{-1} with respect to the reactant energy and that of the highest transition state in the cycloreversion step lies 31.6 kcal mol^{-1} with respect to the same asymptote. This implies that the energy barrier that must be overcome from the metallacyclobutane is higher than 50 kcal mol^{-1}. This is indicative that this process, with this specific set of ligands, would never occur.

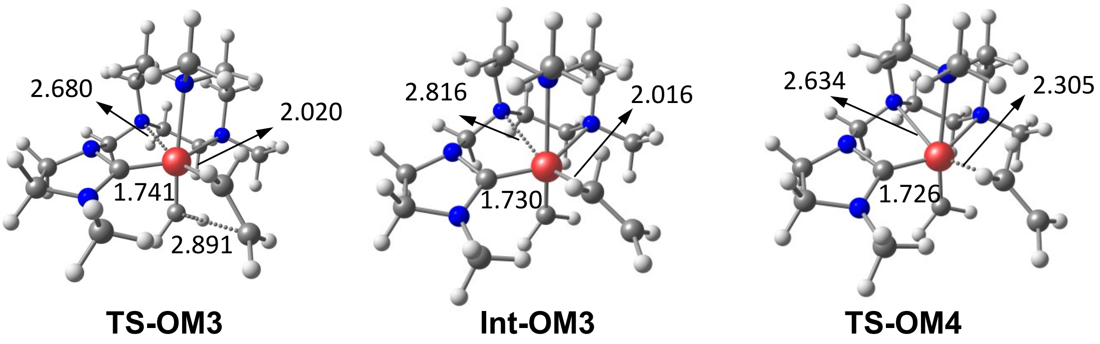

Figure 4. Optimized geometries for ethene metathesis cycloreversion process catalyzed by **5$_0$**. Distances are in Å

Results about the deactivation pathways from **5$_0$** show that both the energy barriers for cyclopropanation from the metallacyclobutane intermediate and those associated with the direct carbene transfer to the olefin have lower Gibbs energy than the transition states associated with the alkene metathesis process. The carbene attack is globally preferred and it presents the triplet state transition state at 26.8 kcal mol^{-1} above reactants. The singlet state transition state lies, slightly higher in energy (29.4 kcal mol^{-1} above separated reactants) and spontaneously evolves towards the formation of an allyl hydride intermediate, which is an intermediate that has also been associated to deactivation processes in olefin metathesis.[92,93]

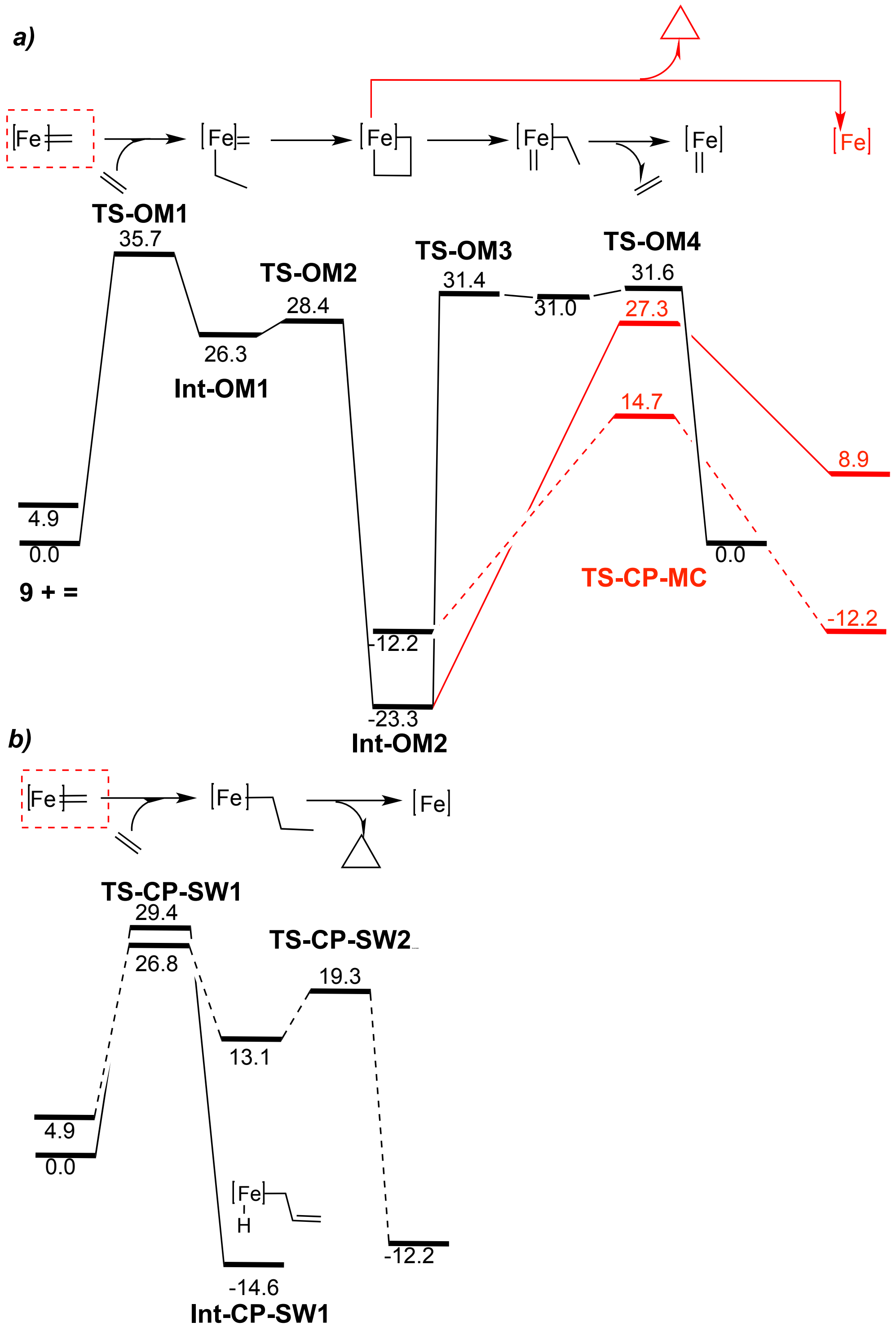

Figure 5. Gibbs energy profile (in kcal mol^{-1}) for the reaction of **9** with ethene: a) alkene metathesis (black) and alkene cyclopropanation involving the metallacyclobutane intermediate; b) alkene cyclopropanation through the stepwise mechanism arising from the carbene extraction by the olefin. Solid lines are used for the singlet (S=0) state and dashed ones for the triplet (S=1) state.

In summary, neither complex **$4_{CeqOtrans}$** nor **5_0** appear to be good candidates for olefin metathesis, despite their thermodynamics. For **$4_{CeqOtrans}$**, the fact that cycloreversion takes place *trans* to the ether group leads to moderate Gibbs energy barriers (~22 kcal mol^{-1}) that are higher than for cyclopropanation. For **5_0**, results suggest that its reaction with olefins would be unlikely and lead to cyclopropanation through carbene extraction mainly in the triplet state, the highest energy barrier being 26.8 kcal mol^{-1}. The generally high energy barriers associated with **5_0** can be explained by formal electron counting. Indeed, **5_0** is an 18 electron complex and thus, it is not prone to accept the coordination of the olefin. This explanation is further confirmed when comparing the results for **5_0** with the reactivity of the analogous Fe(II) complex **5** with ethene (see Figures S16 and S17 of the ESI). In the case of **5**, the initial carbene has 16 electrons and thus, the reaction pathway for metallacyclobutane formation shows the traditional cycloaddition step characterized by lower Gibbs energy barriers (from 35.7 to 13.1 kcal mol^{-1}).

Overall, results show that the addition of σ-donating ligands in formally Fe(II) $L_4Fe{=}CH_2$ complexes[79] leads to carbene species with a singlet ground state. However, the presence of these σ-donating ligands does not guarantee the formation of a singlet state metallacyclobutane intermediate. This arises from the fact that the resulting species present only four d electrons in an octahedral environment, which preferentially leads to a triplet ground state. Only when the octahedral environment is sufficiently distorted the singlet state was found to be the most stable one. This is the case of complexes **4_{Otrans}** **$4_{PeqOtrans}$** and **$4_{CeqOtrans}$**, which show thermodynamic properties close to the Grubbs catalyst. Alternatively, metal reduction to Fe(0) leads to d^6 singlet state octahedral metallacycles and destabilizes cyclopropanation products in the singlet state. The results obtained with the unsymmetric Fe(II) complexes and the Fe(0) carbenes are close to those computed for the efficient second generation Grubbs catalyst. Unfortunately, the energy barriers for the cycloreversion step from the metallacycle are moderate for the representative example of the first set and very high for the second set, suggesting that the alkene metathesis with these complexes is prevented by kinetics. In fact, the selected Fe(II) species present a weak σ-donating ligand *trans* to the olefin that is being released and although this is crucial for thermodynamically preventing the alkene cyclopropanation, it is also well known that strongly undermines cycloreversion.[89–91] Similarly, the Fe(0) $L_4Fe{=}CH_2$ carbenes are formally 18 electron complexes and thus, olefin coordination is strongly compromised. In this context, the use of labile ligands, which would coordinate to the metal in the carbene and the metallacyclobutane to stabilize the singlet state but that could decoordinate during the metathesis process without a large energy cost could potentially be a good strategy for the two types of complexes.

Conclusions

Alkene metathesis is an important reaction in organic synthesis, which is typically catalyzed by d^0 and Ru based metal carbenes. However, the substitution of Mo, W or Ru with most abundant and less toxic first row transition metal complexes is a desirable goal, iron being of particular interest. Here, DFT (OPBE)-D2 calculations were used to analyze the influence of ancillary ligands, coordination around the metal center and the iron formal oxidation state on the multiplicity of the carbene ground state and its reactivity towards olefins. Special attention was devoted to the competition between alkene metathesis and the usually easier alkene cyclopropanation reaction. For that, several complexes based on ligands already used in the synthesis of iron complexes as well as other ones designed *in-silico* for covering borderline cases have been considered. In each case, the singlet, triplet and quintet spin states have been computed for reactants, products and metallacyclobutane intermediate.

Results show that the addition of σ-donating ligands leads to a singlet ground state for the iron carbene. However, when the carbene has a formally Fe(II) metal center[79] the addition of σ-donating ligands is not sufficient for achieving a singlet metallacyclobutane intermediate. This arises from the fact that the metal center in the metallacyclobutane (formally Fe(IV)) has only four d electrons and the ground state of a high field ideal octahedron is the triplet one. Therefore, only in the presence of ligands characterized by very different σ-donating abilities, the metallacyclobutane can be found in a singlet ground state. Complexes with weak σ-donating ligands *trans* to the carbene are of particular interest, since they present a singlet ground state both for the carbene and the metallacycle and the cyclopropanation is less favorable than metathesis. Besides, iron reduction to formally Fe(0) in the carbene also leads to singlet ground state both for the carbene and the metallacyclobutane intermediate and destabilizes the alkene cyclopropanation at least in the singlet state. In fact, the resulting thermodynamics for methathesis and cyclopropanation of some of the $L_4Fe(0)=CH_2$ carbene species considered here are close to those of the efficient Grubbs second generation catalyst. Regrettably, the energy barriers for olefin metathesis of most promising candidates are higher than those for cyclopropanation. This is attributed to the fact that the suitable Fe(II) has a too weak σ-donating ligand *trans* to the olefin that is being released in the cycloreversion step and that the $L_4Fe(0)=CH_2$ complexes are formally eighteen electron complexes and thus, the alkene coordination to them is unfavorable. In this way, the potential use of labile ligands could be of interest since their coordination could stabilize the carbene and the metallacyclobutane singlet state. However, an easy decoordination of this ligand could allow the cycloaddition process to occur. Overall, the here reported data and that reported previously by us on tetracoordinated complexes[44] suggests that there are no general rules for obtaining an *in-silico* designed iron carbene complex with the appropriate preference for alkene metathesis. In fact, the role of the ancillary ligands appears to be strongly related to the coordination number and the formal metal oxidation state.

The authors declare no competing financial interests

Acknowledgements. The authors gratefully acknowledge financial support from MINECO (CTQ2014-59544-P and CTQ2017-89132-P) and the Generalitat de Catalunya (2014SGR-482). EBS gratefully thanks the PhD fellowship from the brazilian funding agency CNPq (245931/2012). XSM is grateful for the Professor Agregat Serra Húnter position.

Supporting Information. The supporting information including the comparison between B3LYP and OPBE energetics; the spin densities, Wiberg bond orders and AIM based delocalization indexes of all carbenes; the energetics of the bridged carbene isomers; the optimized geometries of selected minima and transition states; the schematic molecular orbital diagrams of ML_5 square based pyramid s triplet state carbenes; Gibbs energy profile associated with the reactivity of **5** with ethene and the Cartesian coordinates of all minima and transition state reported along the text is available free of charge on the ACS Publications website.

References

(1) Grubbs, R. H. *Adv. Synth. Catal.* **2007**, *349*, 34–40.

(2) Chauvin, Y. *Angew. Chem. Int. Ed.* **2006**, *45*, 3740–3747.

(3) Schrock, R. R. *Angew. Chem. Int. Ed.* **2006**, *45*, 3748–3759.

(4) Hoveyda, A. H.; Zhugralin, A. R. *Nature* **2007**, *450*, 243–251.

(5) Nomura, K.; Hou, X. *Dalt. Trans.* **2017**, *46*, 12–24.

(6) Mol, J. C. *J. Mol. Catal. A* **2004**, *213*, 39–45.

(7) Biermann, U.; Bornscheuer, U.; Meier, M. A. R.; Metzger, J. O.; Schäfer, H. J. *Angew. Chem. Int. Ed.* **2011**, *50*, 3854–3871.

(8) Jean-Louis Hérisson, P.; Chauvin, Y. *Die Makromol. Chemie* **1971**, *141*, 161–176.

(9) Schrock, R. R. *Chem. Rev.* **2009**, *109*, 3211–3226.

(10) Schrock, R. R.; Hoveyda, A. H. *Angew. Chem. Int. Ed.* **2003**, *42*, 4592–4633.

(11) Murdzek, J. S.; Schrock, R. R. *Organometallics* **1987**, *6*, 1373–1374.

(12) Schaverien, C. J.; Dewan, J. C.; Schrock, R. R. *J. Am. Chem. Soc.* **1986**, *108*, 2771–2773.

(13) Vougioukalakis, G. C.; Grubbs, R. H. *Chem. Rev.* **2010**, *110*, 1746–1787.

(14) Sandford, M. S.; Love, J. A.; Grubbs, R. H. *J. Am. Chem. Soc.* **2001**, *123*, 6543–6554.

(15) Trnka, T. M.; Grubbs, R. H. *Acc. Chem. Res.* **2001**, *34*, 18–29.

(16) Nguyen, S. T.; Grubbs, R. H.; Ziller, J. W. *J. Am. Chem. Soc.* **1993**, *115*, 9858–9859.

(17) Schwab, P.; Grubbs, R. H.; Ziller, J. W. *J. Am. Chem. Soc.* **1996**, *118*, 100–110.

(18) Scholl, M.; Ding, S.; Lee, C. W.; Grubbs, R. H. *Org. Lett.* **1999**, *1*, 953–956.

(19) Hou, X.; Nomura, K. *J. Am. Chem. Soc.* **2016**, *138*, 11840–11849.

(20) Hou, X.; Nomura, K. *J. Am. Chem. Soc.* **2015**, *137*, 4662–4665.

(21) Castarlenas, R.; Esteruelas, M. A.; Oñate, E. *Organometallics* **2005**, *24*, 4343–4346.

(22) Tebbe, F. N.; Parshall, G. W.; Ovenall, D. W. *J. Am. Chem. Soc.* **1979**, *101*, 5074–5075.

(23) Chirik, P.; Morris, R. *Acc. Chem. Res.* **2015**, *48*, 2495.

(24) Su, B.; Cao, Z. C.; Shi, Z. J. *Acc. Chem. Res.* **2015**, *48*, 886–896.

(25) Louie, J.; Grubbs, R. H. *Organometallics* **2001**, *20*, 481–484.

(26) Brookhart, M.; Studabaker, W. B. *Chem. Rev.* **1987**, *87*, 411–432.

(27) Liu, J.; Hu, L.; Wang, L.; Chen, H.; Deng, L. *J. Am. Chem. Soc.* **2017**, *139*, 3876–3888.

(28) Zhu, S.-F.; Zhou, Q.-L. *Natl. Sci. Rev.* **2014**, *1*, 580–603.

(29) Vasiliu, M.; Arduengo, A. J.; Dixon, D. A. *J. Phys. Chem. C* **2014**, *118*, 13563–13577.

(30) Brookhart, M.; Tucker, J. R.; Husk, G. R. *J. Am. Chem. Soc.* **1981**, *103*, 979–981.

(31) Brookhart, M.; Tucker, J. R.; Husk, G. R. *J. Am. Chem. Soc.* **1983**, *105*, 258–264.

(32) Klose, A.; Solari, E.; Floriani, C.; Re, N.; Chiesi-Villa, A.; Rizzoli, C. *Chem. Commun.* **1997**, No. 23, 2297–2298.

(33) Esposito, V.; Solari, E.; Floriani, C.; Re, N.; Rizzoli, C.; Chiesi-Villa, A. *Inorg. Chem.* **2000**, *39*, 2604–2613.

(34) Poignant, G.; Nlate, S.; Guerchais, V.; Edwards, A. J.; Raithby, P. R. *Organometallics* **1997**, *16*, 124–132.

(35) Hamaker, C. G.; Mirafzal, G. A.; Woo, L. K. *Organometallics* **2001**, *20*, 5171–5176.

(36) Li, Y.; Huang, J.-S.; Zhou, Z.-Y.; Che, C.-M.; You, X.-Z. *J. Am. Chem. Soc.* **2002**, *124*, 13185–13193.

(37) Du, G.; Andrioletti, B.; Rose, E.; Woo, L. K. *Organometallics* **2002**, *21*, 4490–4495.

(38) Edulji, S. K.; Nguyen, S. T. *Organometallics* **2003**, *22*, 3374–3381.

(39) Chen, Y.; Zhang, X. P. *J. Org. Chem.* **2007**, *72*, 5931–5934.

(40) Lindley, B. M.; Swidan, A.; Lobkovsky, E. B.; Wolczanski, P. T.; Adelhardt, M.; Sutter, J.; Meyer, K. *Chem. Sci.* **2015**, *6*, 4730–4736.

(41) Russell, S. K.; Hoyt, J. M.; Bart, S. C.; Milsmann, C.; Stieber, S. C. E.; Semproni, S. P.; DeBeer, S.; Chirik, P. J. *Chem. Sci.* **2014**, *5*, 1168–1174.

(42) Conde, A.; Sabenya, G.; Rodríguez, M.; Postils, V.; Luis, J. M.; Díaz-Requejo, M. M.; Costas, M.; Pérez, P. J. *Angew. Chem. Int. Ed.* **2016**, *55*, 6530–6534.

(43) Eisenstein, O.; Hoffmann, R.; Rossi, A. R. *J. Am. Chem. Soc.* **1981**, *103*, 5582–5584.

(44) De Brito Sá, É.; Rodríguez-Santiago, L.; Sodupe, M.; Solans-Monfort, X. *Organometallics* **2016**, *35*, 3914–3923.

(45) Poater, A. *Catal. Commun.* **2014**, *44*, 2–5.

(46) Poater, A.; Pump, E.; Vummaleti, S. V. C.; Cavallo, L. *Chem. Phys. Lett.* **2014**, *610–611*, 29–32.

(47) Poater, A.; Vummaleti, S. V. C.; Pump, E.; Cavallo, L. *Dalt. Trans.* **2014**, *43*, 11216–11220.

(48) Mauksch, M.; Tsogoeva, S. B. *Chem. - A Eur. J.* **2017**, *23*, 10264–10269.

(49) Handy, N. C.; Cohen, A. J. *Mol. Phys.* **2001**, *99*, 403–412.

(50) Cohen, A. J.; Handy, N. C. *Mol. Phys.* **2001**, *99*, 607–615.

(51) Perdew, J. P.; Burke, K.; Ernzerhof, M. *Phys. Rev. Lett.* **1996**, *77*, 3865–3868.

(52) Francl, M. M.; Pietro, W. J.; Hehre, W. J.; Binkley, J. S.; Gordon, M. S.; DeFrees, D. J.; Pople, J. A. *J. Chem. Phys.* **1982**, *77*, 3654–3665.

(53) Hariharan, P. C.; Pople, J. A. *Theor. Chim. Acta* **1973**, *28*, 213–222.

(54) Frisch, M. J.; Pople, J. A.; Binkley, J. S. *J. Chem. Phys.* **1984**, *80*, 3265–3269.

(55) Krishnan, R.; Binkley, J. S.; Seeger, R.; Pople, J. A. *J. Chem. Phys.* **1980**, *72*, 650–654.

(56) Grimme, S. *J. Comput. Chem.* **2006**, *27*, 1787–1799.

(57) Frisch, M. J.; Trucks, G. W.; Schlegel, H. B.; Scuseria, G. E.; Robb, M. A.; Cheeseman, J. R.; Scalmani, G.; Barone, V.; Mennucci, B.; Petersson, G. A.; Nakatsuji, H.; Caricato, M.; Li, X.; Hratchian, H. P.; Izmaylov, A. F.; Bloino, J.; Zheng, G.; Sonnenberg, J. L.; Hada, M.; Ehara, M.; Toyota, K.; Fukuda, R.; Hasegawa, J.; Ishida, M.; Nakajima, T.; Honda, Y.; Kitao, O.; Nakai, H.; Vreven, T.; Montgomery Jr., J. A.; Peralta, J. E.; Ogliaro, F.; Bearpark, M.; Heyd, J. J.; Brothers, E.; Kudin, K. N.; Staroverov, V. N.; Kobayashi, R.; Normand, J.; Raghavachari, K.; Rendell, A.; Burant, J. C.; Iyengar, S. S.; Tomasi, J.; Cossi, M.; Rega, N.; Millam, J. M.; Klene, M.; Knox, J. E.; Cross, J. B.; Bakken, V.; Adamo, C.; Jaramillo, J.; Gomperts, R.; Stratmann, R. E.; Yazyev, O.; Austin, A. J.; Cammi, R.; Pomelli, C.; Ochterski, J. W.; Martin, R. L.; Morokuma, K.; Zakrzewski, V. G.; Voth, G. A.; Salvador, P.; Dannenberg, J. J.; Dapprich, S.; Daniels, A. D.; Farkas, Ö.; Foresman, J. B.; Ortiz, J. V; Cioslowski, J.; Fox, D. J. p Gaussian, Inc., Wallingford CT, 2009.

(58) Reed, A. E.; Curtiss, L. A.; Weinhold, F. *Chem. Rev.* **1988**, *88*, 899–926.

(59) Bader, R. F. W. *Chem. Rev.* **1991**, *91*, 893–928.

(60) Swart, M.; Groenhof, A. R.; Ehlers, A. W.; Lammertsma, K. *J. Phys. Chem. A* **2004**, *108*, 5479–5483.

(61) Swart, M. *J. Chem. Theory Comput.* **2008**, *4*, 2057–2066.

(62) Kiawi, D. M.; Bakker, J. M.; Oomens, J.; Buma, W. J.; Jamshidi, Z.; Visscher, L.; Waters, L. B. F. M. *J. Phys. Chem. A* **2015**, *119*, 10828–10837.

(63) de Brito Sá, É.; Rimola, A.; Rodríguez-Santiago, L.; Sodupe, M.; Solans-Monfort, X. *J. Phys. Chem. A* **2018**, DOI:10.1021/acs.jpca.7b11656.

(64) Harvey, J. N. *Annu. Reports Sect. "C" (Physical Chem.* **2006**, *102*, 203–226.

(65) Company, A.; Gómez, L.; Güell, M.; Ribas, X.; Luis, J. M.; Que, L.; Costas, M. *J. Am. Chem. Soc.* **2007**, *129*, 15766–15767.

(66) Font, D.; Canta, M.; Milan, M.; Cussó, O.; Ribas, X.; Klein Gebbink, R. J. M.; Costas, M. *Angew. Chem. Int. Ed.* **2016**, *55*, 5776–5779.

(67) Olivo, G.; Cussó, O.; Costas, M. *Chem. - An Asian J.* **2016**, *11*, 3148–3158.

(68) Kernbach, U.; Ramm, M.; Luger, P.; Fehlhammer, W. P. *Angew. Chem. Int. Ed.* **1996**, *35*, 310–312.

(69) Vogel, C.; Heinemann, F. W.; Sutter, J.; Anthon, C.; Meyer, K. *Angew. Chem. Int. Ed.* **2008**, *47*, 2681–2684.

(70) Riener, K.; Haslinger, S.; Raba, A.; Högerl, M. P.; Cokoja, M.; Herrmann, W. A.; Kühn, F. E. *Chem. Rev.* **2014**, *114*, 5215–5272.

(71) Planas, O.; Roldán-Gómez, S.; Martin-Diaconescu, V.; Parella, T.; Luis, J. M.; Company, A.; Ribas, X. *J. Am. Chem. Soc.* **2017**, *139*, 14649–14655.

(72) Optimizations for quintet state metallacyclobutane intermediates spontaneously evolved to cyclopropanation products.

(73) Solans-Monfort, X.; Copéret, C.; Eisenstein, O. *J. Am. Chem. Soc.* **2010**, *132*, 7750–7757.

(74) Solans-Monfort, X.; Copéret, C.; Eisenstein, O. *Organometallics* **2012**, *31*, 6812–6822.

(75) Solans-Monfort, X.; Copéret, C.; Eisenstein, O. *Organometallics* **2015**, *34*, 1668–1680.

(76) Suresh, C. H.; Koga, N. *Organometallics* **2004**, *23*, 76–80.

(77) Paredes-Gil, K.; Solans-Monfort, X.; Rodriguez-Santiago, L.; Sodupe, M.; Jaque, P. *Organometallics* **2014**, *33*, 6065–6075.

(78) de Brito Sá, É.; Rodríguez-Santiago, L.; Sodupe, M.; Solans-Monfort, X. *Organometallics* **2016**, *35*, 3914–3923.

(79) Carbenes are considered as neutral ligands.

(80) Nuñez-Zarur, F.; Solans-Monfort, X.; Rodríguez-Santiago, L.; Sodupe, M. *Organometallics* **2012**, *31*, 4203–4215.

(81) Solans-Monfort, X.; Pleixats, R.; Sodupe, M. *Chem. - A Eur. J.* **2010**, *16*, 7331–7343.

(82) Straub, B. F. *Angew. Chem. Int. Ed.* **2005**, *44*, 5974–5978.

(83) Vyboishchikov, S. F.; Bühl, M.; Thiel, W. *Chem. - A Eur. J.* **2002**, *8*, 3962–3975.

(84) Cavallo, L. *J. Am. Chem. Soc.* **2002**, *124*, 8965–8973.

(85) Correa, A.; Cavallo, L. *J. Am. Chem. Soc.* **2006**, *128*, 13352–13353.

(86) Adlhart, C.; Chen, P. *J. Am. Chem. Soc.* **2004**, *126*, 3496–3510.

(87) Aagaard, O. M.; Meier, R. J.; Buda, F. *J. Am. Chem. Soc.* **1998**, *120*, 7174–7182.

(88) Benitez, D.; Tkatchouk, E.; Goddard III, W. A. *Chem. Commun.* **2008**, *0*, 6194.

(89) Núñez-Zarur, F.; Solans-Monfort, X.; Restrepo, A. *Inorg. Chem.* **2017**, *56*, 10458–10473.

(90) Schinzel, S.; Chermette, H.; Copéret, C.; Basset, J.-M. *J. Am. Chem. Soc.* **2008**, *130*, 7984–7987.

(91) Solans-Monfort, X.; Clot, E.; Copéret, C.; Eisenstein, O. *J. Am. Chem. Soc.* **2005**, *127*, 14015–14025.

(92) Van Rensburg, W. J.; Steynberg, P. J.; Meyer, W. H.; Kirk, M. M.; Forman, G. S. *J. Am. Chem. Soc.* **2004**, *126*, 14332–14333.

(93) Leduc, A. M.; Salameh, A.; Soulivong, D.; Chabanas, M.; Basset, J. M.; Copéret, C.; Solans-Monfort, X.; Clot, E.; Eisenstein, O.; Böhm, V. P. W.; Röper, M. *J. Am. Chem. Soc.* **2008**, *130*, 6288–6297.

Table of Contents Graphic

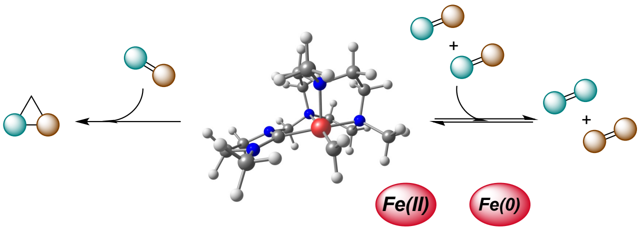

	Fe(II)	Fe(0)
S=0 carbene ground state	✗	✓
preference for metathesis in S=0 state	✗	✓
Olefin metathesis kinetics	✓	✗